Disrupted Resting-State Functional Connectivity in Progressive Supranuclear Palsy

M.C. Piattella, F. Tona, M. Bologna, E. Sbardella, A. Formica, N. Petsas, N. Filippini, A. Berardelli, and P. Pantano

ABSTRACT

BACKGROUND AND PURPOSE: Studies on functional connectivity in progressive supranuclear palsy have been restricted to the thalamus and midbrain tegmentum. The present study aims to evaluate functional connectivity abnormalities of the subcortical structures in these patients. Functional connectivity will be correlated with motor and nonmotor symptoms of the disease.

MATERIALS AND METHODS: Nineteen patients with progressive supranuclear palsy (mean age, 70.93 ± 5.19 years) and 12 age-matched healthy subjects (mean age, 69.17 ± 5.20 years) underwent multimodal MR imaging, including fMRI at rest, 3D T1-weighted imaging, and DTI. fMRI data were processed with fMRI of the Brain Software Library tools by using the dorsal midbrain tegmentum, thalamus, caudate nucleus, putamen, and pallidum as seed regions.

RESULTS: Patients had lower functional connectivity than healthy subjects in all 5 resting-state networks, mainly involving the basal ganglia, thalamus, anterior cingulate, dorsolateral prefrontal and temporo-occipital cortices, supramarginal gyrus, supplementary motor area, and cerebellum. Compared with healthy subjects, patients also displayed subcortical atrophy and DTI abnormalities. Decreased thalamic functional connectivity correlated with clinical scores, as assessed by the Hoehn and Yahr Scale and by the bulbar and mentation subitems of the Progressive Supranuclear Palsy Rating Scale. Decreased pallidum functional connectivity correlated with lower Mini-Mental State Examination scores; decreased functional connectivity in the dorsal midbrain tegmentum network correlated with lower scores in the Frontal Assessment Battery.

CONCLUSIONS: The present study demonstrates a widespread disruption of cortical-subcortical connectivity in progressive supranuclear palsy and provides further insight into the pathophysiologic mechanisms of motor and cognitive impairment in this condition.

ABBREVIATIONS: ACC = anterior cingulate cortex; DLPF = dorsolateral prefrontal cortex; dMT = dorsal midbrain tegmentum; FA = fractional anisotropy; FC = functional connectivity; MD = mean diffusivity; PSP = progressive supranuclear palsy; SMA = supplementary motor area

Progressive supranuclear palsy (PSP) is one of the most common forms of atypical parkinsonism, characterized by early-onset postural instability, falls, and oculomotor abnormalities. Patients with PSP often have cognitive impairment, involving frontal executive functions and language, and behavioral symptoms, including apathy and social withdrawal or disinhibition.[1,2] The pathologic changes in PSP include neuronal degeneration and τ immune-reactive depositions in the basal ganglia, diencephalon, brain stem, and cerebellum, with limited involvement of the neocortex.[3]

MR imaging has detected several structural changes in PSP, which mainly involve the midbrain, thalamus, basal ganglia, frontal cortex, and white matter bundles, reflecting the underlying neurodegenerative processes present in this condition.[4-7] However, the relationship between brain abnormalities and clinical manifestations is still unclear.

The resting-state fMRI technique is a method used to investigate spontaneous neuronal activity at rest.[8] Spontaneous neuronal activity is identified by slow fluctuations in the blood oxygen level–dependent signal and is represented by spatial maps of correlations of these blood oxygen level–dependent signal fluctuations within anatomically separate brain regions, also defined as maps of functional connectivity (FC).[8] FC in PSP has previously been explored in 2 studies with a limited focus on the thalamus[9] and dorsal midbrain tegmentum (dMT) regions.[10] Both studies reported functional disconnection between each of these struc-

Received July 18, 2014; accepted after revision November 11.

From the Department of Neurology and Psychiatry (M.C.P., F.T., E.S., A.F., N.P., A.B., P.P.), Sapienza, University of Rome, Italy; Neuromed Institute Istituto Di Ricovero e Cura a Carattere Scientifico (M.B., A.B., P.P.), Pozzilli, Italy; and Department of Psychiatry and FMRIB Centre (N.F.), University of Oxford, United Kingdom.

Please address correspondence to Maria Cristina Piattella, MD, Department of Neurology and Psychiatry, Sapienza University of Rome, Viale dell'Università, 30-00185 Rome, Italy; e-mail: mcpiattella@gmail.com

http://dx.doi.org/10.3174/ajnr.A4229

tures and some cortical, subcortical, and cerebellar sites.[9,10] It is unknown whether FC abnormalities also affect other key subcortical areas in PSP.[3] Owing to the widespread degeneration of subcortical structures in PSP,[3] the FC of the caudate nucleus, putamen, and pallidum may also be affected in this condition. Due to the basal ganglia involvement in motor and cognitive functions, through the parallel interconnections with the frontal cortex,[11,12] understanding FC abnormalities of the caudate nucleus, putamen, and pallidum in PSP would provide further information on the pathophysiologic mechanisms of the disease. To achieve this goal, we evaluated the FC from the caudate, putamen, and pallidum nuclei, in addition to the thalamus and dMT. The ultimate aim of this article was to investigate possible correlations between cortical-subcortical network disruption and clinical scores of disease severity.

MATERIALS AND METHODS

Subjects

We enrolled 19 patients who were diagnosed with PSP (9 women; mean age, 70.93 ± 5.19 years) according to the National Institute for Neurological Disorders and Society for PSP criteria[13] and were consecutively referred to the Department of Neurology and Psychiatry at the Sapienza University of Rome, between January 2011 and October 2012. All the patients were clinically classified as having Richardson syndrome, one of the subtypes of PSP,[1,14] by experienced neurologists (A.B. and M.B.). Exclusion criteria were other neurologic, psychiatric, and systemic diseases and general contraindications to MR imaging. Patients were clinically evaluated (by A.F.) by using the Unified Parkinson's Disease Rating Scale,[15] the Frontal Assessment Battery,[16] the Hoehn and Yahr Scale,[17] the Mini-Mental State Examination,[18] and the PSP Rating Scale and its subscales.[19] All patients also underwent a multimodal MR imaging study (by M.C.P. and F.T.), which included resting-state fMRI, diffusion tensor imaging, and volumetric imaging. Twelve healthy subjects (9 women; mean age, 69.17 ± 5.20 years) with no history of neurologic or psychiatric disease at the time of the examination constituted the control group.

Participants provided their written informed consent. The study protocol was approved by the institutional review board of Sapienza University of Rome and complied with the Health Insurance Portability and Accountability Act.

MR Imaging Acquisition

A standardized protocol was performed on a 3T scanner (Magnetom Verio; Siemens, Erlangen, Germany). The 12-channel head coil of the manufacturer designed for parallel imaging (generalized autocalibrating partially parallel acquisitions) was used for signal reception. A multiplanar T1-weighted localizer with section orientation parallel to the subcallosal line was acquired at the beginning of each MR imaging examination. The MR imaging protocol included the following sequences for all the subjects: 1) blood oxygen level–dependent single-shot echo-planar images (TR = 3000 ms, TE = 30 ms, flip angle = 89°, FOV = 192, matrix = 64 × 64, 50 axial sections 3-mm -thick, no gap, 120 volumes, acquisition time = 6 minutes 11 seconds), with all patients and healthy subjects being instructed to close their eyes and stay awake during the resting-state fMRI acquisitions; 2) DTI acquired with a single-shot echo-planar spin-echo sequence with 30 directions (TR = 12,200 ms, TE = 94 ms, FOV = 192 mm, matrix = 96 × 96, b = 0 and 1000 s/mm^2, 72 axial sections 2-mm-thick, no gap, acquisition time = 13 minutes 15 seconds); 3) a high-resolution 3D T1-weighted MPRAGE sequence (TR = 1900 ms, TE = 2.93 ms, flip angle = 9 °, FOV = 260 mm, matrix = 256 × 256, 176 sagittal sections 1-mm-thick, no gap, acquisition time = 3 minutes 48 seconds); and 4) dual turbo spin-echo, proton-attenuation, and T2-weighted images (TR = 3320 ms, TE = 10/103 ms, FOV = 220 mm, matrix = 384 × 384, 25 axial sections 4-mm-thick, 30% gap). The dual turbo spin-echo sequences were obtained to exclude subjects with brain alterations due to concomitant diseases.

Image Processing and Data Analysis

Data analysis was carried out by using the fMRI of the Brain Software Library (FSL), Version 4.1.9 (http://www.fmrib.ox.ac.uk/fsl).

Preprocessing. Single-subject preprocessing and group analysis were performed by using the fMRI Expert Analysis Tool, Version 5.98, part of FSL (http://fsl.fmrib.ox.ac.uk/fsl/fslwiki/FEAT). The first 3 volumes of the 120 resting-state blood oxygen level–dependent volumes were discarded to obtain a steady-state of the blood oxygen level–dependent signal. In brief, preprocessing consisted of head-motion correction, brain extraction, spatial smoothing by using a Gaussian kernel of full width at half maximum of 5 mm, and high-pass temporal filtering equivalent to a period of 100 seconds. Functional data were registered to structural images (within-subject) and Montreal Neurological Institute standard space (to allow higher level group comparisons) by using the FMRIB Linear Image Registration Tool (http://www.fmrib.ox.ac.uk/) and Nonlinear Image Registration Tool (http://fsl.fmrib.ox.ac.uk/fsl/fslwiki/FNIRT) and then were optimized by using a boundary-based registration approach.[20]

Functional Connectivity (Seed Description, Time-Series Extraction, and Higher Level Analysis). Individual seed-ROI masks of the thalami, caudate, putamen, and pallidum nuclei were obtained from each subject's high-resolution T1-weighted structural scan by using FMRIB's Integrated Registration and Segmentation Tool (http://fsl.fmrib.ox.ac.uk/fsl/fslwiki/FIRST),[21] an automatic subcortical segmentation program. Each image was visually inspected in the coronal plane to ensure accuracy. Left and right masks of each of the 4 nuclei of interest (thalamus, caudate, putamen, and pallidum) were merged to obtain a single bilateral mask. In addition, a 4-mm-radius spheric ROI was placed on the dMT; it was centered according to the coordinates (5, −15, −8) of a previous study.[10] Each ROI was registered to functional coordinate space and was used to extract the related time course after having preprocessed the raw fMRI data. Time-series were averaged across all voxels for each seed ROI. Each time-series was separately fed into the fMRI Expert Analysis Tool and produced individual participant-level correlation maps of all voxels that were positively or negatively correlated with each of the seeds. Afterward, higher level (group level) analysis was performed by using FMRIB's Local Analysis of Mixed Effects (http://fsl.fmrib.ox.ac.uk/fsl/fslwiki/FEAT).[22] The general linear model was

applied to test for group averages and differences between the 2 groups (patients and controls) by using a 2-sample unpaired *t* test. The Z-statistic images were thresholded by using clusters determined by $Z > 2.3$, and a whole-brain family-wise-error-corrected cluster significance threshold of $P < .05$ was applied to the suprathreshold clusters. Anatomic localization of significant clusters was established according to the Harvard-Oxford Structural Atlas, the Juelich histologic atlas, and the Oxford Thalamic Connectivity Probability Atlas included in the FSL (http://www.fmrib.ox.ac.uk/fsl/data/atlas-descriptions.html).

Nuisance Signal Regression and Covariates of No Interest Included in the Model. To account for potential indeterminate noise,[23,24] we also identified seeds of CSF and white matter on each individual functional EPI, and their time courses were added as covariates of no interest (nuisance) into each of the seed-ROI voxelwise correlation analyses to remove nonneural contributions to the blood oxygen level–dependent signal and thus enhance specificity. Similarly, the age of the study participants and volumes of the specific seeds were entered as nuisance covariates. Finally, structural maps were used as additional covariates on a voxel-by-voxel basis to account for potential gray matter differences. Very briefly, GM images of each subject were extracted by using FMRIB's Integrated Registration and Segmentation Tool,[21] registered in standard space, smoothed to match the fMRI data, demeaned within each group, and added to the model used to analyze fMRI data.

To visualize a unique image common to areas of functional abnormalities shared by the 5 maps of FC, we first performed a transformation of between-group difference maps in binary data; then, we performed a voxel-by-voxel sum of the 5 binarized maps. In the final image, we attributed a different color to each voxel value (range, 0–5). Finally, parameter estimates in individual functional connectivity maps, within a group mask of each of the 5 functional connectivity maps, were used to correlate functional connectivity with both clinical scores and structural damage (brain volumes and DTI parameters) in the patient group.

Structural MR Imaging. T1 3D images were processed by using SIENA/X (part of FSL), a fully automated and accurate method for measuring cross-sectional changes in brain volume.[25] This automated method also provided values of normalized cortical volume.

Subcortical volumes (ie, the caudate, putamen, pallidum, thalamus nuclei, and the brain stem) were estimated through FMRIB's Integrated Registration and Segmentation Tool.[21] Subcortical volumes were corrected for individual differences in intracranial volume by an individual scale factor obtained by SIENA/X.

Diffusion MR Imaging. Eddy current correction was used to preprocess raw DTI images to correct for distortions due to the gradient directions applied. Subsequently, DTIFit, part of FMRIB's Diffusion Toolbox (http://fsl.fmrib.ox.ac.uk/fsl/fsl-4.1.9/fdt/fdt_dtifit.html), was used to fit a diffusion tensor model at each voxel and generate fractional anisotropy (FA), mean diffusivity (MD), axial diffusivity, and radial diffusivity maps. Axial diffusivity was calculated from the eigenvalues in the principal direction of water flow ($\lambda 1$). The 2 minor axes ($\lambda 2$ and $\lambda 3$) were averaged to compute radial diffusivity. The average of all 3 ($\lambda 1$, $\lambda 2$, and $\lambda 3$) eigenvalues was used to calculate MD. Briefly, MD and FA are mainly affected by myelin content and, to a lesser extent, FA, by axonal attenuation,[26] while axial diffusivity and radial diffusivity are considered measures of axonal and myelin integrity, respectively.[27] Voxelwise statistical analysis of FA, MD, radial diffusivity, and axial diffusivity data was performed by using a Tract-Based Spatial Statistics tool (http://fsl.fmrib.ox.ac.uk/fsl/fslwiki/TBSS).[27]

All diffusion and FA maps of patient and healthy subject cohorts were first aligned into a common space by using the Nonlinear Image Registration Tool. The most representative diffusion maps were selected automatically as the target, and diffusion maps of all subjects were nonlinearly registered to this. Following this step, all images were transformed into Montreal Neurological Institute standard space. The mean FA image was generated and thinned to create a mean FA skeleton, which represents the centers of all tracts common to the subjects. Each subject's aligned FA data were then projected onto this skeleton, and the resulting data were fed into voxelwise general linear modeling cross-subject statistics. We used a threshold of 0.2 for creation of a mean FA skeleton to include the major WM tracts but exclude peripheral tracts, which may cause significant intersubject variability and/or partial volume effects with GM and CSF. A voxel-by-voxel permutation nonparametric test (5000 permutations) was used to assess group-related differences by using threshold-free cluster enhancement, which avoids using an arbitrary threshold for the initial cluster formation.[28] In addition to FA data, MD, axial diffusivity, and radial diffusivity were also analyzed by using Tract-Based Spatial Statistics in an analogous fashion. The results were corrected for multiple comparisons and reported at a significance level of $P < .05$.

Statistical Analysis

The statistical analysis was performed by using SPSS software, Version 16.0 (IBM, Armonk, New York). All values are reported as mean ± SD or median and range as appropriate. Unpaired *t* tests and χ^2 tests were used to evaluate any differences between groups, after Bonferroni correction for multiple comparisons.

Correlations between clinical and radiologic variables were investigated by backward stepwise regression.

RESULTS

Demographic, clinical, and radiologic characteristics of the 19 patients with PSP are shown in Table 1. There were no statistically significant differences in age and sex distribution between patients and healthy subjects (Table 1).

Functional Connectivity

The dMT, thalamus, caudate, putamen, and pallidum were chosen as ROIs in both patients and healthy subjects, and the FC patterns were identified in each region (Fig 1). Patients with PSP had lower FC than healthy subjects in all 5 functional connectivity maps (Fig. 2).

FC in the dMT functional connectivity map was significantly reduced in the left dorsolateral prefrontal cortex (DLPF) and supramarginal gyrus, as well as in the pregenual anterior cingulate cortex, bilaterally.

FC in the thalamic functional connectivity map was decreased in the basal ganglia and thalamus, dorsolateral prefrontal cortex,

Table 1: Clinical and radiologic characteristics of 19 patients with PSP and of 12 healthy subjects

	Healthy Subjects[a] (n = 12)	Patients with PSP[a] (n = 19)	P Value[b]
Age (yr)	69.172 ± 5.201	70.933 ± 5.196	.356
Male/female[c]	3/9	10/9	.158
UPDRS	–	27.625 ± 17.952	NA
FAB	–	11.187 ± 3.799	NA
H&Y	–	2.9 ± 1.065	NA
MMSE	29.135 ± 0.8	24.325 ± 3.886	NA
PSPRS	–	35.823 ± 16.994	NA
History	–	7.706 ± 3.820	NA
Mentation	–	3.647 ± 2.597	NA
Bulbar	–	3.117 ± 1.996	NA
Ocular	–	7.706 ± 2.932	NA
Limb	–	4.176 ± 3.486	NA
Gait	–	9.235 ± 5.750	NA
Thalamus V (mm^3)	9.483 ± 0.840	8.005 ± 0.657	<.0001[d]
Caudate V (mm^3)	4.380 ± 0.373	3.962 ± 0.477	.015
Putamen V (mm^3)	5.992 ± 0.472	4.835 ± 0.575	<.0001[d]
Pallidum V (mm^3)	2.404 ± 0.472	1.857 ± 0.293	.0004[d]
Brain stem V (mm^3)	14.906 ± 1.652	12.618 ± 1.603	.0006[d]
Intracranial V (mm^3)	1620.661 ± 163.482	1549.769 ± 114.184	.165
Cortical V (mm^3)	600.423 ± 41.923	576.789 ± 49.823	.167
Mean FA	0.508 ± 0.019	0.441 ± 0.030	<.0001[d]
Mean MD ($mm \times sec^{-2}$) $\times 10^{-3}$	0.689 ± 0.026	0.762 ± 0.030	<.0001[d]
Mean RD ($mm \times sec^{-2}$) $\times 10^{-3}$	0.478 ± 0.029	0.561 ± 0.034	<.0001[d]
Mean AD ($mm \times sec^{-2}$) $\times 10^{-3}$	1.049 ± 0.032	1.154 ± 0.056	<.0001[d]

Note:—UPDRS indicates Unified Parkinson's Disease Rating Scale; FAB, Frontal Assessment Battery; H&Y, Hoehn and Yahr Scale; MMSE, Mini-Mental State Examination; PSPRS, PSP Rating Scale; V, volume (left and right values of subcortical volumes are averaged); RD, radial diffusivity; AD, axial diffusivity; –, not available; NA = not applicable.

[a] Values are reported as mean ± SD.

[b] Differences between groups were assessed by t test.

[c] Differences between groups were assessed by χ^2.

[d] Statistically significant values after Bonferroni correction for multiple comparisons.

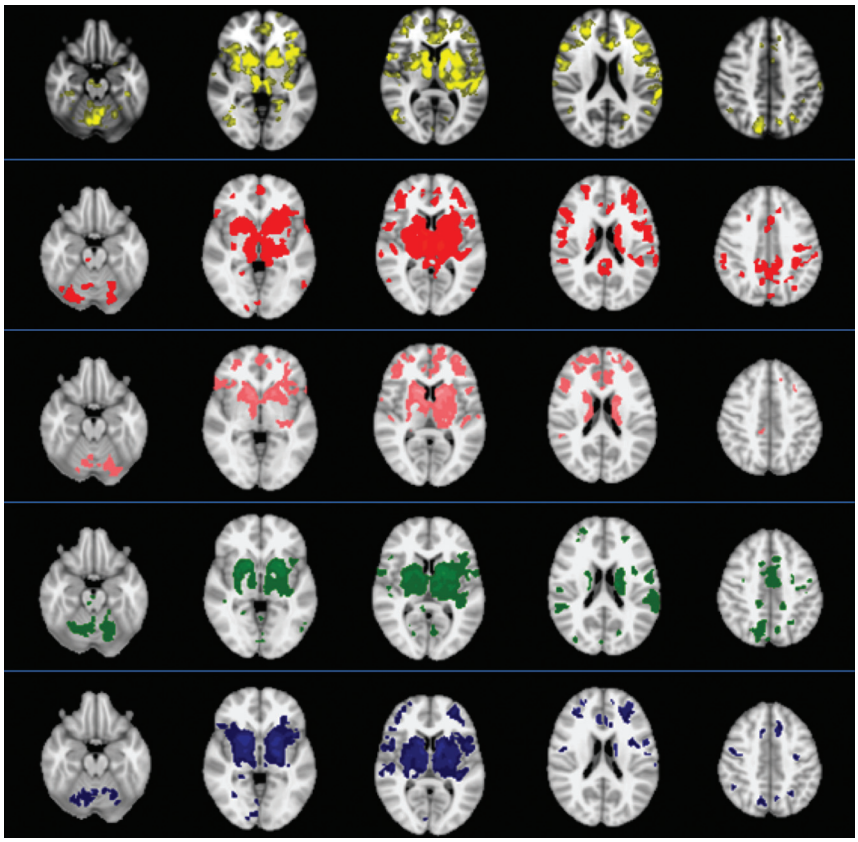

FIG 1. Maps of functional connectivity obtained from 5 seeds, ie, the dorsal midbrain tegmentum (yellow), thalamus (red), caudate (pink), putamen (green), and pallidum (blue)—in 12 healthy subjects (1-sample t test, $P < .05$, corrected for family-wise error). The images are presented according to radiologic orientation.

anterior cingulate cortex (ACC), supplementary motor area (SMA), and precentral gyrus, bilaterally, and in the left temporo-occipital cortex and left cerebellar Crus I.

FC in the caudate nucleus functional connectivity map was significantly lower in clusters located in the thalamus and caudate, ACC, and pre-SMA, bilaterally, and in the left DLPF and temporo-occipital cortex; FC was also decreased in the posterior lobe of the cerebellum (Crus I, lobules VI, VIIb, VIIIa, VIIIb, IX).

FC in the putamen functional connectivity map was significantly reduced in the thalamus and caudate, ACC, SMA, postcentral and supramarginal gyri, precuneus, and temporo-occipital and occipital cortices, bilaterally; the cerebellum was also bilaterally affected (Crus I, Crus II, lobules VI, VIIb, VIIIa, VIIIb, IX).

Finally, FC in the pallidum functional connectivity map was reduced in the basal ganglia and thalamus, DLPF, ACC and SMA, supramarginal gyrus, precuneus, temporo-occipital and occipital cortices, bilaterally, and in the cerebellum (Crus I, lobules VI, VIIb, VIIIa) bilaterally, though to a greater degree on the right side.

To identify common brain areas having reduced FC across all 5 functional connectivity maps, we overlapped results obtained from each map separately (Fig 3). We obtained images showing voxels of significantly decreased FC in 4 results (located in the thalamus, caudate, and ACC, bilaterally, and the left DLPF and temporo-occipital cortex) and in 3 results (located in the left supramarginal gyrus and in the SMA and cerebellar Crus I, lobules VI, VIIb and VIIIb, bilaterally). No focus of decreased FC in any of the 5 functional maps was identified.

Structural Damage

Patients with PSP had significantly lower subcortical structure volumes than healthy subjects, whereas no significant difference emerged between the 2 groups in cerebral cortex volumes (Table 1).

Patients also had significantly lower mean FA and significantly higher MD, radial diffusivity, and axial diffusivity values than healthy subjects (Table 1).

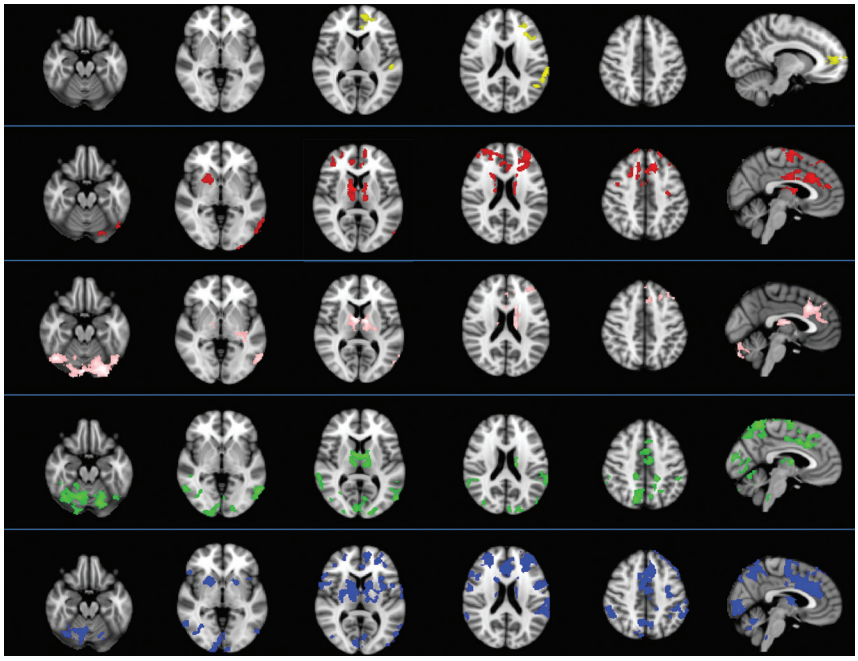

FIG 2. Differences between 19 patients with progressive supranuclear palsy and 12 healthy subjects in functional connectivity obtained from 5 seeds (2-sample *t* test, $P < .05$, corrected for family-wise error). Patients with PSP had significantly lower FC than healthy subjects in all 5 FC maps—that is, the dorsal midbrain tegmentum (yellow), thalamus (red), caudate (pink), putamen (green), and pallidum (blue). The images are presented according to radiologic orientation.

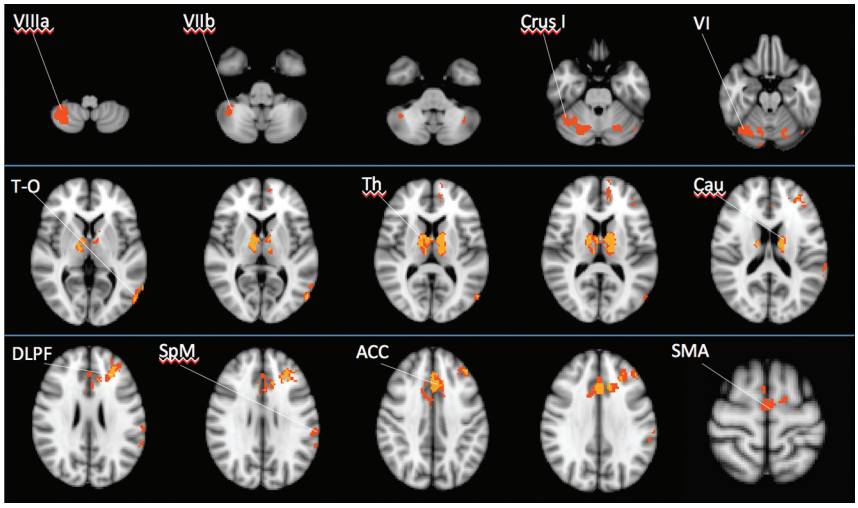

FIG 3. Images showing common areas of functional abnormalities shared by the 5 maps of FC. Different colors show the number of abnormal FC maps: in yellow, voxels of decreased FC in 4 maps; and in orange, voxels of decreased FC in 3 maps. Voxels of decreased FC in 2 maps are not shown. No focus of decreased FC in any of the 5 maps was identified. The images are presented according to radiologic orientation.

Correlation Analysis

FC estimates did not correlate with regional subcortical volumes and DTI parameters. The correlation analysis between the parameter estimates of FC within each of the 5 functional connectivity maps and clinical measures, as assessed by the Unified Parkinson's Disease Rating Scale, Frontal Assessment Battery, Hoehn and Yahr scale, Mini-Mental State Examination, and PSP Rating Scale and its subscales, yielded significant results (Table 2). Estimates of thalamic FC were inversely correlated with the Hoehn and Yahr Scale and the bulbar and mentation subitems of the PSP Rating Scale scores ($P \leq .05$). Estimates of pallidum FC were directly correlated with Mini-Mental State Examination scores ($P = .03$), and estimates of the dMT FC were directly correlated with Frontal Assessment Battery scores ($P = .04$). Overall, these results indicated that decreased FC was associated with more severe manifestations of the disease. Conversely, regional subcortical volumes and DTI parameters did not correlate with clinical scores of disease severity.

DISCUSSION

The main finding of this study is that all the networks we evaluated—dMT, thalamus, caudate, putamen, and pallidum—exhibited lower FC in patients with PSP than in healthy subjects in several subcortical and cortical areas. Cortical disconnection mainly involved the frontal cortex (DLPF, ACC, SMA, precentral gyrus) and parietal (supramarginal gyrus and precuneus), temporal, and occipital cortices; the basal ganglia, thalamus, and cerebellum were also affected. Disruption of specific brain regions (ie, the thalamus, caudate, ACC, SMA, and cerebellum on both sides and the DLPF, temporo-occipital cortex, and supramarginal gyrus on the left side) was a common finding in the various functional connectivity maps analyzed.

Following a previous observation by Gardner et al,[10] who first found reduced dMT FC in the cerebellum, thalamus, striatum, and frontal and parietal cortices in patients with PSP, in the present study, we provide further evidence showing that FC in the dMT functional connectivity map is reduced in the left DLPF and supramarginal gyrus and in the pregenual anterior cingulated cortex, bilaterally. Moreover, in the present study, we did not find any region of enhanced dMT FC, which is in keeping with previous results.[10] With regard to thalamic FC, we confirmed the reduced connectivity in the premotor cortex, SMA, thalamus, basal ganglia, and cerebellum previously described by Whitwell et al[9] in patients with PSP. Unlike us, however, they did not detect decreased FC in the ACC and found increased FC in regions surrounding the perisylvian fissure.[9] These discrepancies between the 2 studies are likely due to differences in the methodology used for the data analysis or in the selection of patients or both.

Table 2: Significant correlations between parameter estimates of FC maps and clinical scores in patients with PSP

	Clinical Scales[a]	β	*P* Value	95% CI	R^2
Thalamus	Bulbar	−5.89	.04	−11.57 to −0.20	0.19
Thalamus	Mentation	−8.02	.05	−16.20 to −0.15	0.27
Thalamus	H&Y	−3.51	.03	−6.60 to −0.40	0.53
Pallidum	MMSE	12.23	.03	1.19–23.27	0.52
dMT	FAB	42.16	.04	2.24–82.08	0.26

Note:—FAB indicates Frontal Assessment Battery; H&Y, Hoehn and Yahr Scale; MMSE, Mini-Mental State Examination.

[a] Bulbar and Mentation are subitems of the PSP Rating Scale.

With respect to the previous studies,[9,10] we evaluated FC also from the caudate nucleus, putamen, and pallidum and found that functional disruption was a consistent finding in PSP and extensively involved multiple subcortical and cortical areas. The thalamus, caudate, ACC, DLPF, and SMA are part of the parallel circuits that connect the basal ganglia and frontal cortex and are implicated in motor and cognitive functions,[29,30] with the putamen mainly being connected to motor cortical areas[12] and the caudate nucleus mainly being involved in cognitive frontal circuits.[30] The decrease in thalamic FC we observed in all the functional connectivity maps, with the exception of the dMT, highlights the key role of the thalamus, which is an important integration center of networks related to emotional, cognitive, and motor functions[31] in the pathophysiology of PSP. We also observed that the FC was abnormal in a specific region of the ACC in all the functional connectivity maps, with the exception of the dMT. This finding supports the concept of an overlap between different domains (ie, motor, cognitive, and emotional functions in the ACC).[30,32] The DLPF, which plays a key role in executive functions,[33] was disconnected from the thalamus and pallidum bilaterally and from the dMT and caudate on the left side alone. This asymmetric FC likely reflects hemispheric functional specialization in executive functions between the left and right DLPF.[34] Last, the SMA was disconnected in the putamen, pallidum, and thalamic functional connectivity maps, while a region in the medial superior frontal cortex corresponding to the pre-SMA[35] was disconnected in the caudate functional connectivity map. The functional alterations we observed are in agreement with anatomic interconnections among the putamen, SMA, and motor cortices on 1 side and among the caudate, pre-SMA, and prefrontal cortex on the other side.[35,36]

In addition to areas belonging to the subcortical-frontal circuits, the decrease in FC was consistently observed in the cerebellum and in the left temporo-occipital cortex and supramarginal gyrus, thereby suggesting a functional involvement of connections between basal ganglia and cortical areas other than frontal ones in the pathophysiology of PSP. The basal ganglia receives projections from widespread regions of the cerebral cortex, including the parietal and temporal lobes.[37] Furthermore, although the main interactions between the basal ganglia–cortical and cerebellum-cortical loops occur largely at the cortical level,[33] recent evidence points to direct connections between the cerebellum and basal ganglia.[38,39]

In this study, patients with PSP displayed a gray matter volume decrease in subcortical structures and DTI abnormalities in white matter compared with healthy subjects, which is in keeping with the results of previous studies.[5-7] These structural abnormalities did not correlate with FC. Although it is commonly assumed that FC reflects structural connectivity, the relationship between the 2 is rather complex[40]: FC can be observed, for example, between regions with no or few anatomic connections, owing to the dynamic reorganization capabilities of functional connections in the brain.[41]

Regarding the clinical impact of MR imaging structural abnormalities, previous studies that investigated possible relationships between cerebral atrophy measurements and disease severity generally failed to detect a significant correlation.[5,9] There are few reports of correlations between regional measurements of DTI parameters and clinical scores.[42] In the present study, neither regional brain volumes nor mean DTI metrics correlated with the clinical severity of patients with PSP. These observations suggest that the severity of clinical impairment may be due to a functional disruption of subcortical-cortical circuits rather than to structural abnormalities. To evaluate the effects of functional abnormalities on clinical severity, we investigated a possible correlation between disease severity clinical scores and parameter estimates of FC. We observed that thalamic FC was associated with both motor and cognitive abnormalities, as shown by correlations with Hoehn and Yahr Scale scores and with the bulbar and mentation subitems of the PSP Rating Scale; the pallidum FC correlated with the Mini-Mental State Examination and the dMT FC correlated with Frontal Assessment Battery changes. This latter finding is in keeping with the significant relationship between FC of the dMT network and the severity of cognitive impairment, found by Gardner et al.[10] The present observations suggest that FC abnormalities in PSP might be developed as surrogate biomarkers of motor and cognitive abnormalities in PSP.

This study has certain limitations. First, we used a seed-based analysis, which is intrinsically flawed from a methodologic point of view owing to the a priori choice of the brain areas to correlate with the rest of the brain.[8] Second, the seeds of our study included each of the 5 subcortical structures as a whole, with no distinction being made between the various components and nuclei. This drawback is related to the spatial resolution of the blood oxygen level–dependent images, which is insufficient to yield a reliable parcellation. Third, because we studied a homogeneous group of patients affected by Richardson syndrome,[1] and not by other PSP subtypes, the conclusion of our study cannot be extended to other subtypes of PSP. Last, we did not perform a follow-up study; therefore, further investigations are needed to clarify whether FC abnormalities in PSP are useful measures to predict the clinical outcome in this condition.

CONCLUSIONS

Our data on PSP clearly point to widespread functional alterations involving 5 different functional connectivity maps. Some of these abnormalities are strictly correlated with the severity of clinical impairment, suggesting that the characterization of patterns and dynamics of brain networks may shed light on pathophysiologic and clinical changes in patients with PSP.

Disclosures: Nikolaos Petsas—*UNRELATED*: *Consultancy*: Federazione Italiana Sclerosi Multipla (fellowship).* Patrizia Pantano—*UNRELATED*: *Grants/Grants Pending*: Federazione Italiana Sclerosi Multipla.* *Money paid to the institution.

REFERENCES

1. Colosimo C, Bak TH, Bologna M, et al. **Fifty years of progressive supranuclear palsy.** *J Neurol Neurosurg Psychiatry* 2014;85:938–44
2. Steele JC, Richardson JC, Olszewski J. **Progressive supranuclear palsy: a heterogeneous degeneration involving the brain stem, basal ganglia and cerebellum with vertical gaze and pseudobulbar palsy, nuchal dystonia and dementia.** *Arch Neurol* 1964;10:333–59
3. Dickson DW, Ahmed Z, Algom AA, et al. **Neuropathology of variants of progressive supranuclear palsy.** *Curr Opin Neurol* 2010;23:394–400
4. Quattrone A, Nicoletti G, Messina D, et al. **MR imaging index for differentiation of progressive supranuclear palsy from Parkinson disease and the Parkinson variant of multiple system atrophy.** *Radiology* 2008;246:214–21
5. Saini J, Bagepally BS, Sandhya M, et al. **Subcortical structures in progressive supranuclear palsy: vertex-based analysis.** *Eur J Neurol* 2013;20:493–501
6. Shi HC, Zhong JG, Pan PL, et al. **Gray matter atrophy in progressive supranuclear palsy: meta-analysis of voxel-based morphometry studies.** *Neurol Sci* 2013;34:1049–55
7. Stamelou M, Knake S, Oertel WH, et al. **Magnetic resonance imaging in progressive supranuclear palsy.** *J Neurol* 2011;258:549–58
8. Fox MD, Raichle ME. **Spontaneous fluctuations in brain activity observed with functional magnetic resonance imaging.** *Nat Rev Neurosci* 2007;8:700–11
9. Whitwell JL, Avula R, Master A, et al. **Disrupted thalamocortical connectivity in PSP: a resting-state fMRI, DTI, and VBM study.** *Parkinsonism Relat Disord* 2011;17:599–605
10. Gardner RC, Boxer AL, Trujillo A, et al. **Intrinsic connectivity network disruption in progressive supranuclear palsy.** *Ann Neurol* 2013;73:603–16
11. Alexander GE, Crutcher MD, DeLong MR. **Basal ganglia-thalamocortical circuits: parallel substrates for motor, oculomotor, "prefrontal" and "limbic" functions.** *Prog Brain Res* 1990;85:119–46
12. Bonelli RM, Cummings JL. **Frontal-subcortical circuitry and behavior.** *Dialogues Clin Neurosci* 2007;9:141–51
13. Litvan I, Agid Y, Calne D, et al. **Clinical research criteria for the diagnosis of progressive supranuclear palsy (Steele-Richardson-Olszewski syndrome): report of the NINDS-SPSP international workshop.** *Neurology* 1996;47:1–9
14. Williams DR, Lees AJ. **Progressive supranuclear palsy: clinicopathological concepts and diagnostic challenges.** *Lancet Neurol* 2009;8:270–79
15. Goetz CG, Fahn S, Martinez-Martin P, et al. **Movement Disorder Society-sponsored revision of the Unified Parkinson's Disease Rating Scale (MDS-UPDRS): process, format, and clinimetric testing plan.** *Mov Disord* 2007;22:41–47
16. Dubois B, Slachevsky A, Litvan I, et al. **The FAB: a Frontal Assessment Battery at bedside.** *Neurology* 2000;55:1621–26
17. Hoehn MM, Yahr MD. **Parkinsonism: onset, progression, and mortality.** *Neurology* 1998;50:318
18. Folstein MF, Folstein SE, McHugh PR. **"Mini-mental state": a practical method for grading the cognitive state of patients for the clinician.** *J Psychiatr Res* 1975;12:189–98
19. Golbe LI, Ohman-Strickland PA. **A clinical rating scale for progressive supranuclear palsy.** *Brain* 2007;130(pt 6):1552–65
20. Greve DN, Fischl B. **Accurate and robust brain image alignment using boundary-based registration.** *Neuroimage* 2009;48:63–72
21. Patenaude B, Smith SM, Kennedy DN, et al. **A Bayesian model of shape and appearance for subcortical brain segmentation.** *Neuroimage* 2011;56:907–22
22. Woolrich MW, Behrens TE, Smith SM. **Constrained linear basis sets for HRF modelling using variational Bayes.** *Neuroimage* 2004;21:1748–61
23. Gavrilescu M, Shaw ME, Stuart GW, et al. **Simulation of the effects of global normalization procedures in functional MRI.** *Neuroimage* 2002;17:532–42
24. Macey PM, Macey KE, Kumar R, et al. **A method for removal of global effects from fMRI time series.** *Neuroimage* 2004;22:360–66
25. Smith SM, Zhang Y, Jenkinson M, et al. **Accurate, robust, and automated longitudinal and cross-sectional brain change analysis.** *Neuroimage* 2002;17:479–89
26. Song SK, Sun SW, Ramsbottom MJ, et al. **Dysmyelination revealed through MRI as increased radial (but unchanged axial) diffusion of water.** *Neuroimage* 2002;17:1429–36
27. Smith SM, Jenkinson M, Johansen-Berg H, et al. **Tract-based spatial statistics: voxelwise analysis of multi-subject diffusion data.** *Neuroimage* 2006;31:1487–505
28. Smith SM, Nichols TE. **Threshold-free cluster enhancement: addressing problems of smoothing, threshold dependence and localisation in cluster inference.** *Neuroimage* 2009;44:83–98
29. DeLong MR, Wichmann T. **Circuits and circuit disorders of the basal ganglia.** *Arch Neurol* 2007;64:20–24
30. Alexander GE, DeLong MR, Strick PL. **Parallel organization of functionally segregated circuits linking basal ganglia and cortex.** *Annu Rev Neurosci* 1986;9:357–81
31. Haber SN, Calzavara R. **The cortico-basal ganglia integrative network: the role of the thalamus.** *Brain Res Bull* 2009;78:69–74
32. Paus T. **Primate anterior cingulate cortex: where motor control, drive and cognition interface.** *Nat Rev Neurosci* 2001;2:417–24
33. Middleton FA, Strick PL. **Cerebellar projections to the prefrontal cortex of the primate.** *J Neurosci* 2001;21:700–12
34. Kaller CP, Rahm B, Spreer J, et al. **Dissociable contributions of left and right dorsolateral prefrontal cortex in planning.** *Cereb Cortex* 2011;21:307–17
35. Zhang S, Ide JS, Li CR. **Resting-state functional connectivity of the medial superior frontal cortex.** *Cereb Cortex* 2012;22:99–111
36. Kim JH, Lee JM, Jo HJ, et al. **Defining functional SMA and pre-SMA subregions in human MFC using resting state fMRI: functional connectivity-based parcellation method.** *Neuroimage* 2010;49:2375–86
37. Middleton FA, Strick PL. **The temporal lobe is a target of output from the basal ganglia.** *Proc Natl Acad Sci U S A* 1996;93:8683–87
38. Hoshi E, Tremblay L, Féger J, et al. **The cerebellum communicates with the basal ganglia.** *Nat Neurosci* 2005;8:1491–93
39. Wu T, Hallett M. **The cerebellum in Parkinson's disease.** *Brain* 2013;136(pt 3):696–709
40. Damoiseaux JS, Greicius MD. **Greater than the sum of its parts: a review of studies combining structural connectivity and resting-state functional connectivity.** *Brain Struct Funct* 2009;213:525–33
41. O'Reilly JX, Croxson PL, Jbabdi S, et al. **Causal effect of disconnection lesions on interhemispheric functional connectivity in rhesus monkeys.** *Proc Natl Acad Sci U S A* 2013;110:13982–87
42. Wang J, Wai Y, Lin W-Y, et al. **Microstructural changes in patients with progressive supranuclear palsy: a diffusion tensor imaging study.** *J Magn Reson Imaging* 2010;32:69–75